Hindawi
Mathematical Problems in Engineering
Volume 2020, Article ID 7210547, 7 pages
https://doi.org/10.1155/2020/7210547

Research Article

Feature Analysis on Mixed Traffic Flow of Manually Driven and Autonomous Vehicles Based on Cellular Automata

Xinghua Hu,[1] **Mengyu Huang**,[1] **and Jianpu Guo**[2]

[1]*School of Traffic and Transportation, Chongqing Jiaotong University, Chongqing 400074, China*
[2]*Chongqing Productivity Promotion Center, Chongqing 401147, China*

Correspondence should be addressed to Xinghua Hu; xhhoo@cqjtu.edu.cn

Received 17 August 2020; Revised 25 September 2020; Accepted 23 October 2020; Published 6 November 2020

Academic Editor: Hussein Abulkasim

This paper attempts to disclose the features of the mixed traffic flow of manually driven vehicles (MVs) and autonomous vehicles (AVs). Considering dynamic headway, the mixed traffic flow was modelled based on the improved single-land cellular automata (CA) traffic flow model (DHD) proposed by Zhang Ningxi. The established CA model was adopted to obtain the maximum flow of the mixed traffic flow and was analyzed under different proportions of AVs. On this basis, the features of the mixed traffic flow were summarized. The main results are as follows: the proportion of AVs has a significant impact on the mixed traffic flow; when the proportion reached 0.6, the flow of the whole lane was twice that of the MV traffic flow. At a low density, the AV proportion has an obvious influence on mixed traffic flow. At a high density, the mixed traffic flow changed very little, as the AV proportion increased from 0 to 5. The reason is that the flow of the whole lane is constrained by the fact that MVs cannot move faster. However, when the AV proportion reached 0.8, the flow of the whole lane became three times that at the proportion of 0.6. At the speed of 126 km/h, the flow rate was 2.5 times the speed limit of 54 km/h. The findings lay a theoretical basis for the modelling of multilane mixed traffic flow.

1. Introduction

In traffic engineering, the traffic flow model is an important research tool to facilitate the understanding of complex traffic phenomena. For more than half a century, many have theorized the traffic flow of manually driven vehicles (MVs), creating numerous traffic flow models and traffic flow prediction models [1–5]. Among them, the traffic flow model based on cellular automata (CA) stands out for its abilities to reproduce various complex phenomena in the traffic flow system and reflect the features of traffic flow.

In recent years, artificial intelligence (AI) and machine learning (ML) have made rapid progress [6, 7]. Thanks to the constant updates of algorithms and sensing techniques, autonomous vehicles (AVs) are poised to make up an important part of road traffic. In addition to their excellence in driving, AVs may bring a huge impact on the safety and efficiency of the operation of the traffic system [8–10]. However, the proportion of AVs will be limited early after their deployment. MVs and AVs are expected to travel together on roads for a long period of time.

The mixture of MVs and AVs will complicate the features of the traffic flow, which originally only involves MVs. The Institute of Electrical and Electronic Engineers (IEEE) predicted that the AV proportion will reach 75% by 2040. With the advancement of autonomous driving technology, the growth in the number of AVs will gradually pick up speed, due to their ultrashort reaction delay, low requirement for spacing or headway, and broad spectrum of speed. The mixed traffic flow of MVs and AVs will exert an enormous influence on the traditional road traffic system.

So far, only a few scholars have explored the mixed traffic flow of MVs and AVs. In 2003, Bose and Ioannou [11] analyzed the flow densities of MVs and AVs and discussed the shock waves in the mixed traffic flow, using the car following model and the semiautomatic vehicle model. Davis [12] applied the car following model to simulate the traffic phenomena of the mixed traffic flow in the confluence area of the ramp, evaluated the local stability of traffic flow in the presence of AVs, and suggested AVs be provided with interconnected information, such as to debottleneck the traffic congestion on the reduced road. Kim and Liu [13] presented the concept of cooperative autonomous driving, which provides the drivers with the traffic situation ahead, enabling them to make better decisions that favor the efficiency and safety of traffic flow.

Through modelling, Levin and Boyles [10] found that AVs improve the traffic pattern in links and intersections, and the degree of improvement depends on the proportion of such vehicles. However, Levin's model only takes account of the driver's reaction time, without considering the interaction between MVs and AVs. Sharma et al. [14] and van Lint et al. [15] simulated the driving behavior of drivers in the mixed traffic flow model and identified the features of mixed traffic flow but failed to measure the restriction effect of MVs on AVs. Ngoduy [16] noticed the significant improvement to the capacity of the traffic system and travel time, when the AV proportion in the mixed traffic flow reached 30%.

In China, Jiang and Wu [17] were the first to propose a single-land CA model involving AVs. However, Jiang's model retains the random deceleration step reflecting the psychological changes of the driver, causing fluctuations to the speed of AVs. Inspired by Gipps' safety distance rule, Qiu et al. [18] put forward a CA model for AVs based on safety distance. Through simulation, Qin et al. [19] learned that the traditional traffic flow became more stable with the growing proportion of AVs. Liu et al. [20] set up a vehicle following model and proved that connected vehicles improve the stability of traffic flow. Many other simulation experiments [21–25] agree that introducing AVs to the road greatly improves the traffic flow and free flow speed, and the degree of improvement increases with the AV proportion.

Our research is based on the improved single-land CA traffic flow model (DHD) proposed by Zhang et al. [26]. The DHD assumes that daredevil and skillful drivers will resort to dynamic headway to adjust speed and follow the front car. The DHD model can simulate free flow, synchronous flow, and wide-range motion congestion in traffic flow, indicating that synchronous flow will also occur where there is no traffic bottleneck. The AVs, fully controlled by a computer, are similar to vehicles driven by the daredevil drivers in the DHD. In this paper, the mixed traffic flow of MVs and AVs is modelled based on the CA, in the light of the dynamic headway. After that, the maximum flow of the mixed traffic flow was analyzed under different proportions of AVs. In this way, the authors summarized the features of the mixed traffic flow.

2. Modelling

2.1. Motion Rules of MVs. CA traffic flow model is very popular because of its simplicity and ease of computer operation. One of the most important CA traffic flow models is the NaSch model proposed by Nagel and Schrekenberg [1] in 1992. Being a random single-lane CA traffic flow model, the NaSch model regards the lane as a pattern of one-dimensional (ID) discrete lattice points with a length of L and assumes that N vehicles are randomly distributed on the lane. At each moment, a lattice point is either empty or occupied by a vehicle. The state of each vehicle is characterized by its speed V_n $(n = 1, 2, \ldots, N)$, which falls within the interval $\{0, 1, 2, \ldots, V_{\max}\}$, where $V_{\max}$ is the maximum allowable speed. The position of the n-th vehicle is represented as X_n. The distance between the n-th vehicle and the $n+1$ previous vehicles is represented as $d_n = X_{n+1} - X_n - 1$. From t to $t+1$, the position and state of all vehicles are updated in parallel at each time step by the following rules:

Step 1. Acceleration: $V_n(t+1) = \min(V_n(t) + 1, V_{\max})$

Step 2. Deterministic deceleration: $V_n(t+1) = \min(V_n(t), d_n(t))$

Step 3. Probabilistic random deceleration: $V_n(t+1) = \max(V_n(t) - 1, 0)$

Step 4. Position updates: $X_n(t+1) = X_n(t) + V_n(t+1)$

Albeit its simplicity, the NaSch model can depict actual traffic phenomena like spontaneous congestion and stop-and-go wave in crowded traffic. In this paper, the motion rules of MVs are the same as those of ordinary drivers in the DHD; that is, the traffic flow evolves in accordance with the NaSch model.

2.2. Motion Rules of AVs. Considering the motions of the front car, the DHD focuses on the change law of the synchronization between the front and rear cars. Unlike the NaSch model, the DHD no longer treats the headway at the current moment as that at the next moment. Let $V_{n-1}(t+1)$ be the expected speed of the front vehicle. Then, Step 2 of the NaSch model can be modified as

$$V_n(t+1) = \min\left(V_n(t), d_n(t) + V_{n-1}(t+1)\right). \qquad (1)$$

In this way, the headway increases from $d_n(t)$ to $d_n(t) + V_{n-1}(t+1)$, setting a rule for high-speed following. Obviously, AVs can follow the front car at a high speed just like daredevil drivers, owing to the numerous sensors onboard and advanced techniques of information processing. Therefore, the DHD was selected as the basis for the motion rules of AVs.

Moreover, Step 3 (probabilistic random deceleration) was deleted, for AVs are completely controlled by computers, which make no uncertain behavior as traditional drivers do [27]. Considering dynamic headway, the motion rules of AVs can be summed up as follows:

Step 1. Acceleration: $V_n(t+1) = \min(V_n(t) + 1, V_{\max})$

Step 2. Deterministic deceleration: $V_n(t+1) = \min(V_n(t), d_n(t) + V_{n-1}(t+1))$

Step 3. Position updates: $X_n(t+1) = X_n(t) + V_n(t+1)$

The AV proportion in the traffic flow was defined as ρ. If $\rho = 1$, the traffic flow is purely AVs that evolve according to the above three steps; if $\rho = 0$, the traffic flow is purely MVs that evolve according to the rules of the NaSch model; if $0 < \rho < 1$, the traffic flow is a mix of MVs and AVs, and the flow change varies with the ρ value.

3. Numerical Simulation

The mixed traffic flow of MVs and AVs on a 5000 m-long single-land road was simulated on MATLAB. The entire road was simulated under periodic boundary condition, and the vehicle density was strictly controlled: once a vehicle leaves the road, it will reenter the road from the starting point. The road was divided into 1000 cells, each of which is 5 m long. The cell length is approximately the average length of a vehicle. Each cell could be empty or occupied by a vehicle.

The vehicle speed was divided into 6 discrete levels: 0, 1, 2, 3, 4, and 5 cell(s) per time step. Level 0 means that the vehicle is at a standstill; level 5 means the vehicle travels across 5 cells in a time step, corresponding to the speed of 90 km/h. For MVs, because human drivers have some random behaviors during driving, they will cause braking measures, and the probability P of random deceleration was set to 0.1.

The traffic flow was initialized randomly for the simulation. N vehicles with different initial speeds and positions were generated on the road. That is, initial position, speed, and vehicle type are completely random. The total density of the road can be calculated as $\rho = N/L$.

3.1. Simulation of MV Traffic Flow. The flow-density diagram of MV traffic flow was plotted. Based on the speed limit $V_{\max} = 5$, the total number of MVs in the lane was determined, and then the density of the lane was obtained. The entire simulation lasted 20,000 time steps. The first 10,000 time steps were removed to eliminate the transient influence. Then, the average speeds of all MVs in each of the next 10,000 time steps were recorded and multiplied with the current density to produce 10,000 flow values. The above operations were repeated at different initial densities to create more points on the flow-density diagram. The flow-density diagram of MV traffic flow is presented in Figure 1.

As shown in Figure 1, the flow of MV traffic flow peaked at the density of 0.16, which corresponds to an actual flow of 1440 veh/h, an optimal density of 32 veh/km, and a critical speed of 45 km/h. The results shown in Figure 1 are consistent with actual traffic flow.

3.2. Simulation of Mixed Traffic Flow. Next, the flow density of the mixed traffic flow of MVs and AVs was simulated at different proportions of AVs. The simulation results are displayed in Figures 2–5.

As shown in Figures 2–5, the maximum possible flow increased with the AV proportion, indicating that introducing AVs can boost the flow of the whole lane. In Figure 2, the flow-density relationship is linear as density changed from 0 to 0.2 (i.e., actual density changed from 0 to 40 veh/km). Hence, the vehicles in the area of density 0–0.2 belong to the free flow state, and 40 veh/h is the critical density under the AV proportion of 0.2.

With the growing AV proportion, the critical density continued to increase. Once the density surpassed the critical density, the flow of the whole lane started to decline gently,

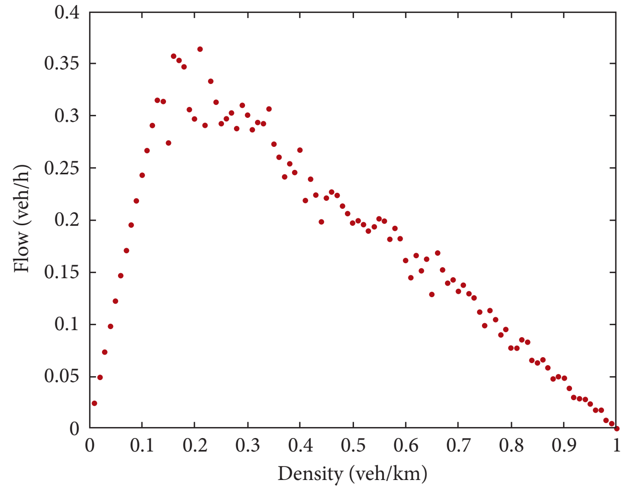

Figure 1: Flow-density diagram of MV traffic flow.

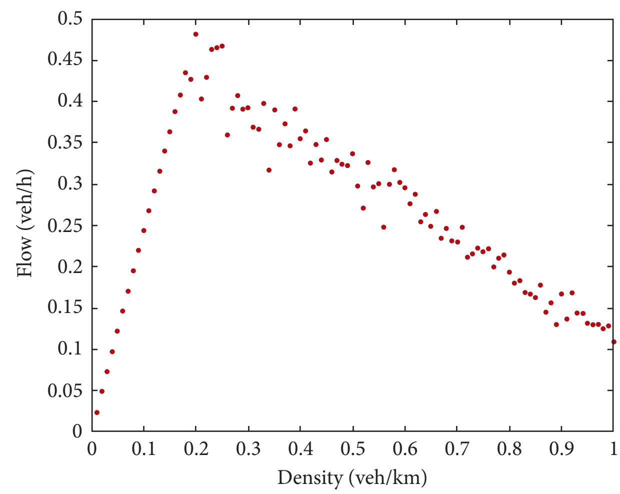

Figure 2: Flow-density diagram of mixed traffic flow at an AV proportion of 0.2.

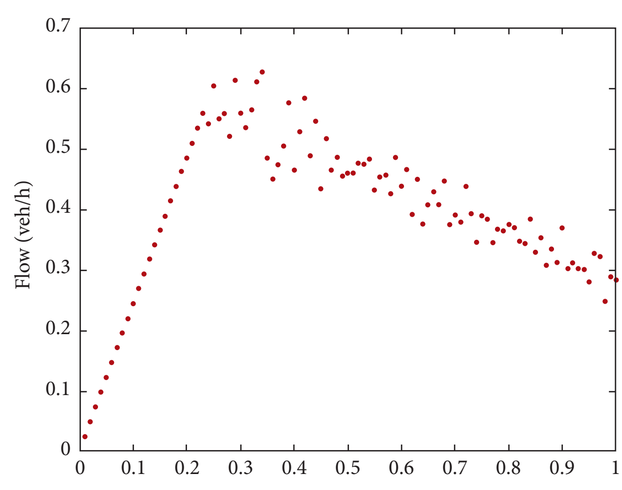

Figure 3: Flow-density diagram of mixed traffic flow at an AV proportion of 0.4.

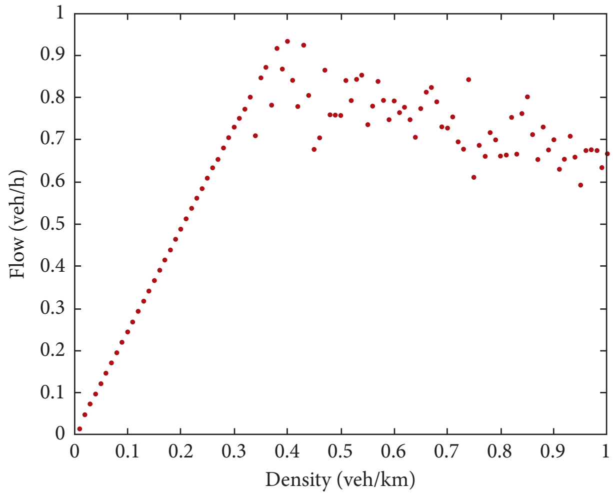

Figure 4: Flow-density diagram of mixed traffic flow at an AV proportion of 0.6.

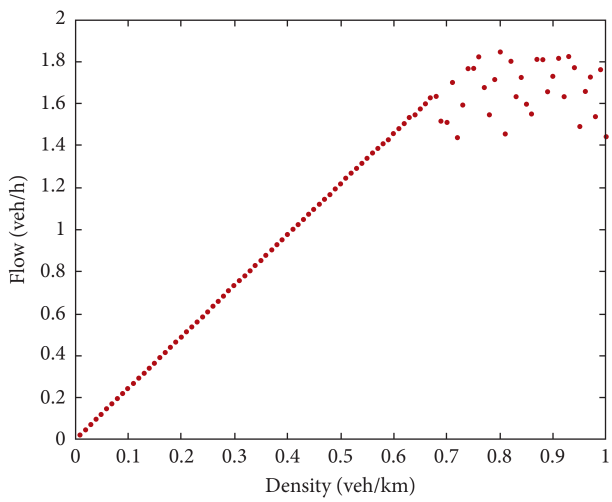

Figure 5: Flow-density diagram of mixed traffic flow at an AV proportion of 0.8.

and the points on the flow-density diagram became scattered. In addition, when the penetration reaches 0.6, the flow of the whole lane was twice that of the MV traffic flow.

3.3. Influence of AV Proportion on Mixed Traffic Flow. Figures 6–10 present the variation of the mixed traffic flow with AV proportions, as the density increased from 0.1 to 0.9 with a step length of 0.2.

As shown in Figures 6–10, the mixed traffic flow was linearly correlated with AV proportion at the density of 0.3; the mixed traffic flow peaked at 2700 veh/h at the AV proportion of 0.6; after AV proportion surpassed 0.6, the mixed traffic flow no longer changed, that is, not correlated with AV proportion. In addition, at the density = 0.9, the mixed traffic flow increased by 2 times, as the AV proportion grew from 0.6 to 0.8.

In our CA model, the AVs receive the expected speed of the front car and gain a wider driving space following the

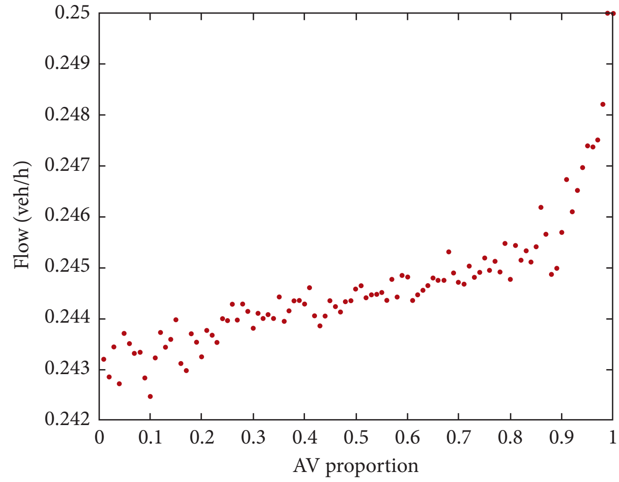

Figure 6: Flow-AV proportion diagram at density = 0.1.

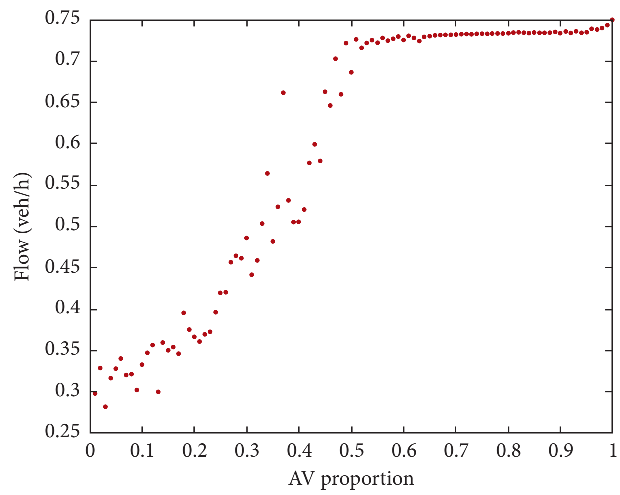

Figure 7: Flow-AV proportion diagram at density = 0.3.

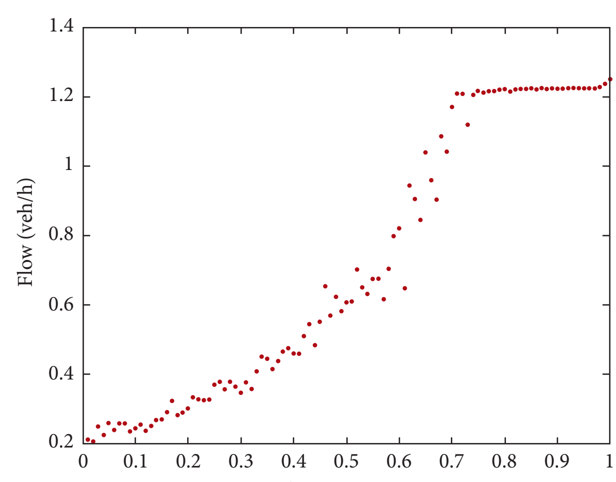

Figure 8: Flow-AV proportion diagram at density = 0.5.

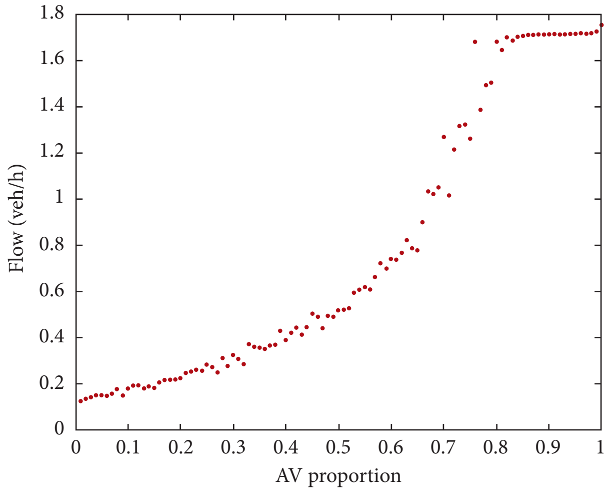

Figure 9: Flow-AV proportion diagram at density = 0.7.

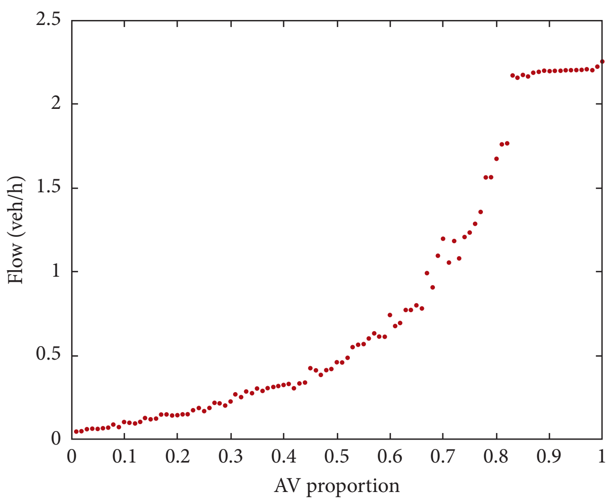

Figure 10: Flow-AV proportion diagram at density = 0.9.

strategy of dynamic headway. Therefore, the AVs can maintain the state of high-speed following. If the front car is an MV, the human driver will experience probabilistic random deceleration. This experience, coupled with the personality of the driver, makes it impossible for the front car to maintain high-speed following. Then, the MV indirectly limits the speed of the AVs behind. The limiting effect is obvious in dense mixed traffic flows with a low AV proportion. As shown in Figures 6–10, when it was smaller than 0.5, the AV proportion has little impact on mixed traffic flow, for the high-speed following of AVs was limited by the huge number of MVs.

If the front car and the rear car are both AVs, the two vehicles will drive on the road like carriages of a train, with a very small space between them, forming a self-organizing fleet in the mixed traffic flow. With the growth in the AV proportion, more and more AVs join the self-organizing fleet, which moves like the uniform flow in fluid mechanics. This explains why the critical density increased with the AV proportion.

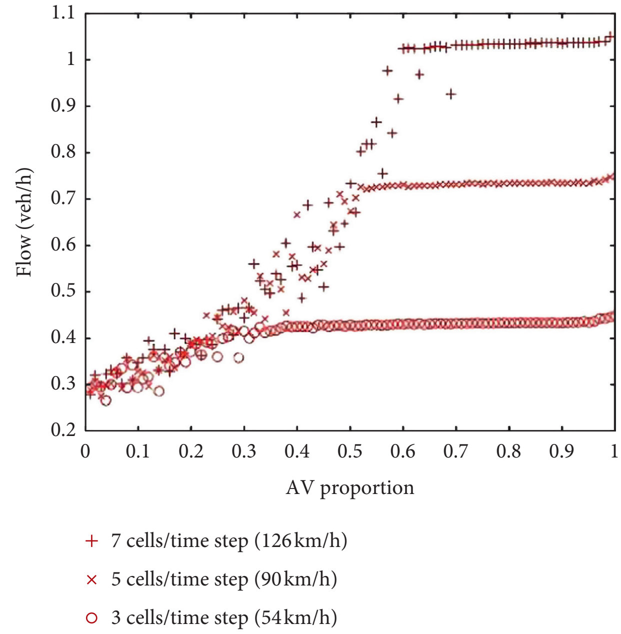

Figure 11: Flow-AV proportion relationship under the three speed limits at density = 0.3.

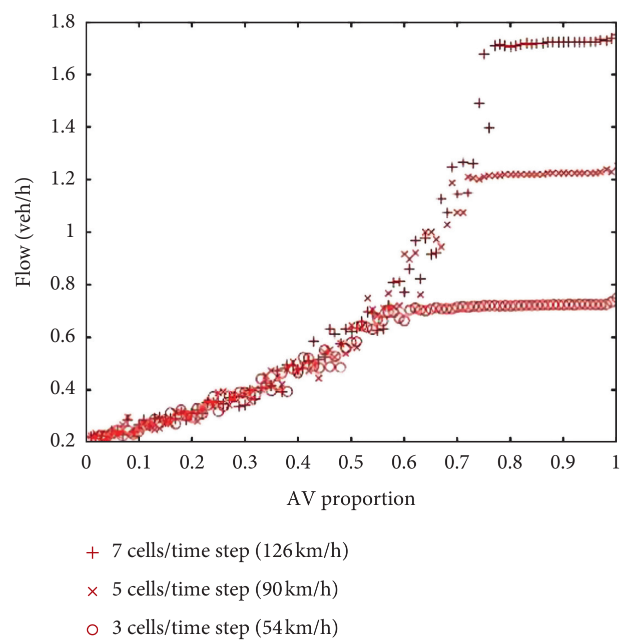

Figure 12: Flow-AV proportion relationship under the three speed limits at density = 0.5.

Focusing on the AV proportions of 0–0.2, the flow of the whole lane was the largest at density $\rho = 0.3$ and relatively small at $\rho = 0.1$ or 0.5. The results are consistent with the three-phase traffic flow theory, indicating that density = 0.5 is closer to the critical density. When the AV proportion fell in 0.6–0.8, the peak flow of the whole lane increased with the density.

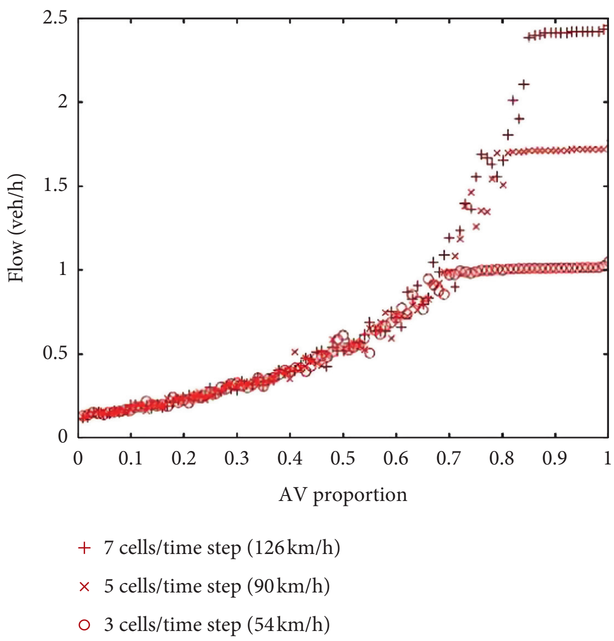

FIGURE 13: Flow-AV proportion relationship under the three speed limits at density = 0.7.

3.4. Influence of Speed Limits on Mixed Traffic Flow. To characterize the mixed traffic flow, different speed limits were introduced to the simulation: 3 cells/time step (54 km/h), 5 cells/time step (90 km/h), and 7 cells/time step (126 km/h). The flow-AV proportion relationships under the three speed limits at different densities are displayed in Figures 11–13, respectively.

As shown in Figures 11–13, regardless of the density, the mixed traffic flow increased with the speed limit. The peak flow under the speed limit of 7 cells/time step was 2.5 times that under 3 cells/time step. When the AV proportion was low, whichever the speed limit, most points in the diagram overlapped each other. This is because MVs are uncertain in driving, failing to maintain high-speed following. Their uncertainties affect the speed of AVs, dragging down the speed of the mixed traffic flow. However, when the AV proportion was high, the speed limit had a serious impact on the simulation results. In this case, the promoting effect of AVs cannot be ignored, while the limiting effect of MVs dwindles.

4. Conclusions

Based on the DHD, this paper designs an improved CA model, in which MVs update their positions by the rules of the NaSch model, while AVs update their positions by the dynamic headway rules. The designed model was applied to MATLAB simulation. The results show that the AV proportion has a significant impact on the mixed traffic flow; when the proportion reached 0.6, the flow of the whole lane was twice that of the MV traffic flow. At a low density, the AV proportion has an obvious influence on mixed traffic flow. At a high density, the mixed traffic flow changed very little, as the AV proportion increased from 0 to 5. However, when the AV proportion reached 0.8, the flow of the whole lane became three times that at the proportion of 0.6. In addition, speed limit also has a major impact on the mixed traffic flow. Regardless of the density, the peak flow under the speed limit of 7 cells/time step (126 km/h) was 2.5 times that under 3 cells/time step (54 km/h).

The proposed model is a single-lane model, in which the motion rules of MVs and AVs are both grounded on the CA. Our model can be extended into a multilane traffic flow model. The application prospect of our model is very broad.

Data Availability

Some or all data, models, or code generated or used during the study are available from the corresponding author by request.

Conflicts of Interest

All the authors do not have any possible conflicts of interest.

References

[1] K. Nagel and M. Schreckenberg, "A cellular automaton model for freeway traffic," *Journal de Physique I*, vol. 2, no. 12, pp. 2221–2229, 1992.

[2] R. Barlovic, L. Santen, A. Schadschneider, and M. Schreckenberg, "Metastable states in cellular automata for traffic flow," *The European Physical Journal B*, vol. 5, no. 3, pp. 793–800, 1998.

[3] V. Kanagaraj and M. Treiber, "Self-driven particle model for mixed traffic and other disordered flows," *Physica A: Statistical Mechanics and its Applications*, vol. 509, pp. 1–11, 2018.

[4] N. Davoodi, A. R. Soheili, and S. M. Hashemi, "A macro-model for traffic flow with consideration of driver's reaction time and distance," *Nonlinear Dynamics*, vol. 83, no. 3, pp. 1621–1628, 2016.

[5] A. I. Delis, I. K. Nikolos, and M. Papageorgiou, "A macroscopic multi-lane traffic flow model for ACC/CACC traffic dynamics," *Transportation Research Record: Journal of the Transportation Research Board*, vol. 2672, no. 20, pp. 178–192, 2018.

[6] W. Meng, C. Mao, J. Zhang, J. Wen, and D. Wu, "A fast recognition algorithm of online social network images based on deep learning," *Traitement du Signal*, vol. 36, no. 6, pp. 575–580, 2019.

[7] U. J. Reddy, B. R. V. R. Reddy, and B. E. Reddy, "Recognition of lung cancer using machine learning mechanisms with fuzzy neural networks," *Traitement du Signal*, vol. 36, no. 1, pp. 87–91, 2019.

[8] A. Talebpour and H. S. Mahmassani, "Influence of connected and autonomous vehicles on traffic flow stability and throughput," *Transportation Research Part C: Emerging Technologies*, vol. 71, pp. 143–163, 2016.

[9] Y.-M. Yuan, R. Jiang, M.-B. Hu, Q.-S. Wu, and R. Wang, "Traffic flow characteristics in a mixed traffic system consisting of ACC vehicles and manual vehicles: a hybrid modelling approach," *Physica A: Statistical Mechanics and its Applications*, vol. 388, no. 12, pp. 2483–2491, 2009.

[10] M. W. Levin and S. D. Boyles, "A multiclass cell transmission model for shared human and autonomous vehicle roads," *Transportation Research Part C: Emerging Technologies*, vol. 62, pp. 103–116, 2016.

[11] A. Bose and P. Ioannou, "Mixed manual/semi-automated traffic: a macroscopic analysis," *Transportation Research Part C: Emerging Technologies*, vol. 11, no. 6, pp. 439–462, 2003.

[12] L. C. Davis, "Improving traffic flow at a 2-to-1 lane reduction with wirelessly connected, adaptive cruise control vehicles," *Physica A: Statistical Mechanics and its Applications*, vol. 451, pp. 320–332, 2016.

[13] S.-W. Kim and W. Liu, "Cooperative autonomous driving: a mirror neuron inspired intention awareness and cooperative perception approach," *IEEE Intelligent Transportation Systems Magazine*, vol. 8, no. 3, pp. 23–32, 2016.

[14] A. Sharma, Y. Ali, M. Saifuzzaman, Z. Zheng, and M. M. Haque, "Human factors in modelling mixed traffic of traditional, connected, and automated vehicles," in *Proceedings of the International Conference on Applied Human Factors and Ergonomics*, pp. 262–273, Los Angeles, CA, USA, July 2017.

[15] H. van Lint, W. Schakel, G. Tamminga, P. Knoppers, and A. Verbraeck, "Getting the human factor into traffic flow models: new open-source design to simulate next generation of traffic operations," *Transportation Research Record: Journal of the Transportation Research Board*, vol. 2561, no. 1, pp. 25–33, 2016.

[16] D. Ngoduy, "Application of gas-kinetic theory to modelling mixed traffic of manual and ACC vehicles," *Transportmetrica*, vol. 8, no. 1, pp. 43–60, 2012.

[17] R. Jiang and Q.-S. Wu, "The adaptive cruise control vehicles in the cellular automata model," *Physics Letters A*, vol. 359, no. 2, pp. 99–102, 2006.

[18] X. P. Qiu, L. N. Ma, X. X. Zhou, and D. Yang, "Research on manual-automatic vehicle mixed traffic flow based on safety distance," *Journal of Transportation Systems Engineering and Information*, vol. 16, no. 4, pp. 101–108, 2016.

[19] Y. Y. Qin, H. Wang, W. Wang, and Q. Wan, "Stability analysis and fundamental diagram of heterogeneous traffic flow mixed with cooperative adaptive cruise control vehicles," *Acta Physica Sinica*, vol. 66, no. 9, Article ID 094502, 2017.

[20] L. Liu, C. Li, Y. Li, S. Peeta, and L. Lin, "Car-following behavior of connected vehicles in a mixed traffic flow: modeling and stability analysis," in *Proceedings of the 2018 IEEE 8th Annual International Conference on CYBER Technology in Automation, Control, and Intelligent Systems (CYBER)*, pp. 1085–1088, Tianjin, China, July 2018.

[21] R. Mohajerpoor and M. Ramezani, "Mixed flow of autonomous and human-driven vehicles: analytical headway modeling and optimal lane management," *Transportation Research Part C: Emerging Technologies*, vol. 109, pp. 194–210, 2019.

[22] A. Ghiasi, O. Hussain, Z. Qian, and X. Li, "A mixed traffic capacity analysis and lane management model for connected automated vehicles: a Markov chain method," *Transportation Research Part B: Methodological*, vol. 106, pp. 266–292, 2017.

[23] Y. Liu, J. Guo, J. Taplin, and Y. Wang, "Characteristic analysis of mixed traffic flow of regular and autonomous vehicles using cellular automata," *Journal of Advanced Transportation*, vol. 2017, Article ID 8142074, 2017.

[24] T. Wietholt and J. Harding, "Influence of dynamic traffic control systems and autonomous driving on motorway traffic flow," *Transportation Research Procedia*, vol. 15, pp. 176–186, 2016.

[25] S. Gong and L. Du, "Cooperative platoon control for a mixed traffic flow including human drive vehicles and connected and autonomous vehicles," *Transportation Research Part B: Methodological*, vol. 116, pp. 25–61, 2018.

[26] N. X. Zhang, H. B. Zhu, H. Lin, and M. Y. Huang, "One-dimensional cellular automaton traffic flow model considering dynamic vehicle spacing," *Acta Physica Sinica*, vol. 64, no. 2, pp. 303–309, 2015.

[27] X. L. Ma, Y. H. Hu, and Q. Y. Yang, "Modeling and simulation of mixed traffic flow in two-lane general vehicle-automatic truck," *Transportation Systems Engineering and Information*, vol. 18, no. 6, pp. 72–80, 2018.